Novel grout material comprised of calcium phosphate compounds: In vitro evaluation of crystal precipitation and strength reinforcement

Masaru Akiyama[a,*], Satoru Kawasaki[b]

[a] Geoscience Research Laboratory Co., Ltd., 1794 Kamiwada, Yamato, Kanagawa 242-0014, Japan

[b] Faculty of Engineering, Hokkaido University, Kita 13, Nishi 8, Kita-ku, Sapporo, Hokkaido 060-8628, Japan

CORRESPONDING AUTHOR: Masaru Akiyama

Geoscience Research Laboratory Co., Ltd., 1794 Kamiwada, Yamato, Kanagawa 242-0014, Japan

E-mail: akiyama@geolab.jp

Telephone number: +81-46-268-7327

Fax number: +81-46-268-7328

ABSTRACT

Calcium phosphate compounds (CPCs) have unique physicochemical properties. As grout material, they afford many advantages such as adequate physical strength, self-setting property, pH dependence of precipitation, non-toxicity, and recyclability. To apply CPCs to the permeability control and reinforcement of ground soil and rock, we explored suitable conditions for in vitro CPC precipitation, conducted unconfined compressive strength (UCS) tests of Toyoura sand test pieces cemented by CPC, and carried out observations and elemental analysis of precipitated CPC crystals. Two kinds of phosphate stock solution and two kinds of calcium stock solution were used to prepare the reaction mixtures, and CPC precipitation was detected in all reaction mixtures. The volume of CPC precipitation in the reaction mixture increased as the pH rose from strongly acidic to around neutral. The UCS of Toyoura sand test pieces cemented by 1.5 M diammonium phosphate and 0.75 M calcium acetate tended to increase with time, reaching a maximum of 63.5 kPa after 14 days of curing. Conversely, the UCS of test pieces cemented by using calcium nitrate was below 20 kPa and showed no significant increase in strength. CPC precipitation with calcium nitrate induced the formation of plate-like crystals, whereas that with calcium acetate induced whisker-like crystals. Elemental analysis of the cemented test pieces showed that the distributions of phosphorus and calcium were similar. The results indicate the practical feasibility of using novel CPC grouts as chemical grouts because of their self-setting property, and as biogrouts because of their crystal

structure and pH dependence of precipitation.

Keywords: Calcium phosphate compound; Grout material; Unconfined compressive strength; Self-setting property; pH dependence; Soil improvement

1. Introduction

In recent years, grout materials that exploit mechanisms of cement material production by microorganisms have been developed for ground permeability control and reinforcement (Whiffin et al., 2007; de Muynck et al., 2010; DeJong et al., 2010; Harkes et al., 2010; Kawasaki et al., 2010). The process of ground improvement by biological action is called “biogrouting” (van Paassen et al., 2009).

Three mechanisms of mineral formation have mainly been considered for biogrouting. One is the precipitation of calcium carbonate by in situ microorganisms and/or added yeasts (Kawasaki et al., 2006). In this process, calcium carbonate is precipitated by the binding of carbonate ions released from microorganisms and calcium ions from the injected grout, which includes calcium and glucose. A second mechanism was reported by Harkes et al. (2010), who used urea instead of glucose and urealytic *Sporosarcina pasteurii* instead of yeast and other in situ microorganisms; the decomposition of urea by *Sporosarcina pasteurii* produced carbon dioxide, which supplied the carbonate ions. In both cases, additional pH buffers or ammonium ions play the role of pH adjuster for effective precipitation. The third mechanism is based on the pH dependence of the extension speed of the siloxane bond; this mechanism was reported by Terajima et al. (2009), who utilized the carbon dioxide produced by yeast to neutralize the alkaline active silica solution because the siloxane bond rapidly extends and gelates in the middle range of pH.

Kawasaki et al. (2006) described the main advantages of using microorganisms in the geotechnical engineering field as follows.

1. Biological cement precipitation is slower than chemical reactions alone. This delay effect, in particular, may enable the technological control of the reaction time.

2. In situ microorganisms are an unused resource in the fields of engineering and rock mechanics. Their use would stimulate the development of novel technologies to lower costs and environmental damage.

Meanwhile, soil and rock vary infinitely in their physical and chemical properties. This fact orients the development of biogrout along two main directions: one, to develop a highly general-purpose biogrout, and the other, to develop a specialized biogrout for a specific kind of soil or rock. To apply biogrout to various soils and rocks, it is very important to increase the number of mechanisms available for the precipitation of cement materials.

In nature, various minerals, such as calcium carbonate, calcium phosphate, calcium oxalate, silicate, and iron oxide, are precipitated by living organisms (Mann, 1988, 1993). These biominerals are promising as engineering materials because they have adequate strength and low environmental impact. In this study, we carried out a fundamental examination on new rock grout materials comprised of calcium phosphate compounds (CPCs) (Fig. 1). CPCs exist as phosphate rocks (mainly fluoroapatite) in the natural environment and as an important inorganic substance (mainly

hydroxyapatite, HA) in living organisms (Dorozhkin and Epple, 2002). There are 11 known CPCs with various calcium-to-phosphate (Ca/P) molar ratios in the ternary system $Ca(OH)_2$-H_3PO_4-H_2O (Table 1). Research and development of materials comprised of CPCs are currently in progress, especially in the fields of medicine and dentistry (e.g., see Martin and Brown, 1995; Bohner et al., 2006; Ginebra et al., 2006).

Medical CPC paste, however, is extremely expensive and has high viscosity, which makes it unfeasible for engineering applications. Therefore, we considered CPC use from an engineering viewpoint and aimed to develop a rock grout material that is precipitated under normal temperature and pressure, with easily handled materials through microbial activity. To the best of our knowledge, no existing rock grout material makes use of the self-setting mechanism of CPC alone or employs microbial pH adjustment activity for CPC precipitation. CPCs have unique physical and chemical properties. Their numerous advantages as a grout material include the following.

1. Gel-like or amorphous CPCs change into HA over time (Fig. 2; Chow, 1991; Tung, 1998). Consequently, CPC hardens after injection into soil and rock because of the self-setting mechanism (Ginebra et al., 1997).

2. The solubility of CPCs depends on the pH of the surrounding environment (Fig. 3; Tung, 1998). This makes it possible to utilize the mechanisms of pH adjustment by microorganisms, which are used in known biogrout methods to control CPC precipitation.

3. Phosphate and calcium stock solutions can be made from fertilizers, and calcium and phosphate can also be extracted from the bones of livestock and the shells of marine animals, respectively.

4. CPCs that precipitate after grout injection are non-toxic.

5. Unlike concrete, re-excavated muck that consists of soil, rock, and CPC grout is recyclable as agricultural fertilizer.

We begin by focusing on the development of novel grout material intended for soil materials (sand, in this study). We then extend our approach to control the strength and permeability of rock materials. This work can contribute to countermeasures for liquefaction in alluvial plains and reclaimed land as well as measures to prevent failure of natural and/or artificial slopes.

In this study, the most suitable conditions for CPC precipitation were determined in an in vitro examination by using phosphate and calcium stock solutions (Step 1 in Fig. 1). Subsequently, test pieces composed of Toyoura sand cemented by CPC were subjected to unconfined compressive strength (UCS) tests and observed by scanning electron microscopy (Step 2 in Fig. 1). Our aim was to evaluate the feasibility of using the novel grout as a chemical grout and a microbiological grout by exploiting the self-setting property of CPC and the microbial pH adjustment activity in CPC precipitation, respectively.

2. Materials and Methods

2.1. In vitro precipitation test of CPC

In this study, reagents with relatively high solubility were chosen for convenient handling during practical application. Monoammonium phosphate (MAP, pH 4.2 (The Merck Index, 2001)) and diammonium phosphate (DAP, pH 8.0 (The Merck Index, 2001)) were used as the components of the phosphate stock solution—a kind of agricultural fertilizer that can be prepared easily. The pH of the phosphate stock solution can be adjusted simply by changing the mixture ratio of MAP and DAP; hence, the components (phosphate ions and ammonium ions) of this material need not be varied to change the pH. To evaluate the effect of pH on the crystal precipitation of CPC, ammonium phosphate (AP) stock solutions with 11 different levels of pH were made by mixing MAP and DAP in proportions ranging from 10:0 to 0:10. For example, if 1 M MAP and 1 M DAP were used, the pH of the 11 resulting solutions ranged from 4.2 (10:0) to 8.4 (0:10). For the calcium stock solution, calcium nitrate (CN) or calcium acetate (CA) was used. All reagents were of special grade (Wako Pure Chemical Industries, Ltd, Osaka).

The reaction mixtures were prepared by mixing the AP solution and one of two calcium solutions at a 1:1 volume ratio (2 mL each); consequently, the final concentrations of the AP and calcium stock solutions were half the initial concentrations. The initial concentrations of the AP and CN solutions were 0.2, 1.0, 2.0, and 3.0 M (the final concentrations were 0.1, 0.5, 1.0, and 1.5 M). A 3.0 M MAP

solution could not be made because the water solubility of MAP at 20 ℃ is 27.2 g/100 g (Kagakubinran, 1993); therefore, a mixture solution of 2 M MAP and 3 M DAP was designated as the 3 M AP stock solution to facilitate the plotting of data even though 2 M MAP was used. The solubility of calcium acetate is 25.8 g/100 g water (20 °C) (Kagakubinran, 1993). As we could not prepare a 2 M solution of calcium acetate, the concentrations of the CA stock solution were set at 0.2, 1.0, and 1.5 M (final concentrations were 0.1, 0.5, and 0.75 M). The in vitro precipitation tests were performed for the entire set of combinations of AP stock solutions and CN (16 reaction mixtures) or CA stock solutions (12 reaction mixtures).

Subsequently, the reaction mixtures were left standing at 20 °C for 2 weeks to monitor their precipitation status; a period of 2 weeks was chosen because changes in this status can appear with time depending on the properties of the CPC. To observe the precipitation status, the proportion of the CPC precipitation volume to the reaction mixture volume (proportion of precipitation volume to reaction mixture, PPR) was measured during this time (the maximum PPR was 1.0). Simultaneously, the pH of the reaction mixture was measured by pHSpear (Eutech Instruments Pte., Ltd., Singapore). This pH device is designed for measuring the pH of solids and semisolids, including gels (e.g., Wilson et al., 2010). The precipitation status was classified into three levels: crystal precipitation (transparent or white solid body), gel precipitation (no crystal precipitation and no deformation when overturned), and fluid precipitation (no crystal precipitation and deformation when overturned).

To evaluate the potential injectability of CPC and its stock solutions, the viscosities of the AP and calcium stock solutions as well as those of the reaction mixtures with the maximum concentration, were measured by using a viscometer (Model DV-I Prime, Brookfield Engineering Laboratories, Inc., Middleboro, MA) according to the manufacturer's protocol.

2.2. UCS test of Toyoura sand test pieces cemented by CPC

Reaction mixtures (sets of each stock solution) for the UCS test were selected according to three criteria, based on the results of the in vitro CPC precipitation test.

Criterion 1: Set of stock solutions with the minimum concentration among reaction mixtures that showed a PPR of 1.0.

Criterion 2: Set of stock solutions with the maximum PPR among those with the maximum concentration.

Criterion 3: Set of stock solutions with a concentration that is closest to average of the concentrations discussed in criteria 1 and 2.

An AP stock solution with an MAP:DAP ratio of 0:10 was used because the combination showed the maximum precipitation among the 11 mixing proportions in each set of selected combinations. Therefore, DAP:CN or DAP:CA represent the combination of the AP stock solution with the CN or CA stock solution, respectively.

Table 2 lists the physical properties of Toyoura sand. To avoid the destruction of the test piece during its removal from the mold, the inner wall of the mold container (φ = 5 cm, h = 10 cm) was covered with a 0.01-cm-thick overhead projector (OHP) sheet. The volumes of the test pieces made by the mold container and maximum volume of the reaction mixture injected into the voids between the Toyoura sand particles were 194.59 cm^3 and 73.3 mL, respectively. According to these values, 36.7 mL each of the DAP and calcium stock solutions were mixed, making their final concentrations half their initial concentrations. Immediately after the reaction mixture was prepared, it was uniformly mixed with weighed Toyoura sand in a stainless-steel ball for two minutes. This mixture was divided into quarters, each of which was placed into a mold with an OHP sheet. The sand in the mold container was tamped down 30 times by a hand rammer after each of the four quarters was placed in the mold. Finally, the edge surface of the test piece was molded flat and covered with Parafilm M (Structure Probe, Inc., West Chester, PA) to avoid desiccation. The test pieces were cured in an airtight container at a high humidity for 1, 7, and 14 days at 20 °C. The UCS of the test pieces removed from the mold container after curing was measured at an axial strain rate of 1 mm/min by the UCS apparatus T266-31100 (Seikensha Co., Ltd., Japan). Two test pieces for each cure time were used in the UCS test.

2.3. Scanning electron microscopy observations and energy dispersive X-ray fluorescence

spectrometer analysis of Toyoura sand test pieces cemented by CPC

Segments of UCS test pieces cemented by the reaction mixture with the maximum PPR value among the sets of AP and calcium stock solutions with the maximum concentration were observed by scanning electron microscopy (SEM) (SuperScan SS-550, Shimadzu Corporation, Kyoto). The segment of the test piece was allowed to dry naturally at 20 ℃ for a few days and was then carbon-coated by using a Quick Carbon Coater (SC-701C, Sanyu Electron Co., Ltd., Tokyo). SEM observations were carried out at an accelerating voltage of 15 kV and at ×2000 magnification. Simultaneously, elemental analyses of test piece segments were carried out by using an energy dispersive X-ray fluorescence spectrometer (EDX) with SEM.

3. Results

3.1. In vitro precipitation test of CPC cemented using CN

CPC precipitation was observed in all reaction mixtures (Fig. 4). The pH of the reaction mixture ranged from 1.6 to 7.5 and showed the highest values among all combinations of AP and CN when the MAP:DAP ratio was 0:10. The PPR showed a tendency to increase with the pH. In the case of 1.5 M CN, the reaction mixtures showed crystal precipitation at all AP concentrations (Fig. 4 A-d, B-d, C-d, and D-d), and the pH was below 4 in all reaction mixtures. In the case of 0.5 M CN, the

PPR of the crystallized reaction mixture was below 0.5. In contrast, most PPRs of gelated reaction mixtures were over 0.5, and more than 0.8 when the AP:CN ratio was 1.5 M:0.5 M (Fig. 4 D-b). In the case of 0.1 M CN, gelated reaction mixtures were observed for all concentrations of AP. Fluid precipitation was observed when the MAP:DAP ratio was 1:9 or 0:10 and the AP:CN ratio was 0.5 M:0.1 M (Fig. 4, B-a).

3.2. In vitro precipitation test of CPC cemented using CA

CPC precipitation was observed in all reaction mixtures (Fig. 5). The pH of the reaction mixture ranged from 4.6 to 7.9. There was no correlation between the PPR and pH values in any set. Crystallization of CPC in all 11 pH steps was observed in only two reaction mixture sets (Fig. 5 A-a and B-b). When the AP:CA ratio was 0.1 M:0.5 M (Fig. 5 A-b) or 0.1 M:0.75 M (Fig. 5 A-c), fluid precipitation was observed in all reaction mixtures. For the six reaction mixture sets with AP concentrations over 1.0 M, a higher pH caused gelated precipitation (Fig. 5 columns C and D). In addition, four reaction mixture sets with AP concentrations over 1.0 M and CA concentrations over 0.5 M showed PPR values over 0.9 in almost all gelated reaction mixtures (Fig. 5 C-b, C-c, D-b, and D-c). Furthermore, the PPR of gelated precipitation was larger than that of crystal precipitation in all cases.

3.3 Viscosity of stock solutions and reaction mixtures

Each of the single stock solutions (DAP, MAP, CN, and CA) at maximum concentration in this study showed a viscosity below 5.0 cps (Fig. 6). When MAP or DAP were mixed with CA, the viscosity of the reaction mixture was similar (~100 cps). In the case of CN, the viscosity of the mixture with MAP (2.5 cps) was significantly different from that with DAP (around 500 cps).

3.4. UCS test

In this study, Toyoura sand test pieces cemented by six reaction mixture sets were chosen based on the results of an in vitro precipitation test (Fig. 7). The measured UCS in this study ranged from 10.2 to 63.5 kPa. The maximum value was measured when the DAP:CA ratio was 1.5 M:0.75 M (Fig. 5 D-c and Fig. 7 F). The UCS tended to increase with the cure time. Test pieces with a DAP:CA ratio of 1 M:0.5 M showed a UCS of over 20 kPa without any tendency to increase with cure time. The UCS values of the other four reaction mixtures were below 20 kPa and showed neither increasing nor decreasing trends as a function of cure time. The test pieces with a DAP:CA ratio of 1.5 M:0.75 M exhibited a stress (σ)-strain (ε) curve with a clear peak around 1.6%, which was shifted leftward relative to those of other combinations (Fig. 8).

3.5. Observation by SEM and elemental analysis by EDX

Segments of UCS test pieces cemented by the reaction mixture with the maximum PPR among the set of AP and calcium stock solutions with the maximum concentration were observed by scanning electron microscopy (Fig. 7 C and F). In images captured at ×76 magnification, particles of Toyoura sand were covered with precipitation in both CN and CA stock solutions (Fig. 9 A and D). In images captured at ×600 magnification, bridges built between particles of Toyoura sand by precipitation were observed (Fig. 9 B and E). At ×2000 magnification, plate-like crystals of ~10 μm in diameter were observed in the segment cemented by CN stock solution (Fig. 9 C). In contrast, a collection of whisker-like precipitations was formed in the segment cemented by CA stock solution (Fig. 9 F). Through elemental analysis, it was found that the distributions of phosphorous and calcium overlapped and corresponded to the distribution of precipitation in the SEM images (Fig. 10).

4. Discussion

4.1. Relationship between CPC precipitation and pH of reaction mixture

The results of an in vitro CPC precipitation test showed that the PPR tended to increase as the pH increased from strongly acidic to around neutral. Apparently, this is why the solubility of the CPC becomes low at around neutrality and in a weakly alkaline region (Tung, 1998). The Ca/P molar ratios in all reaction mixtures of each set were constant regardless of pH, except for 1.5 M AP (each

D column in Fig. 4 and 5). This indicates the possibility that pH-increasing actions including microbial activity, e.g., urea hydrolysis of *Sporosarcina pasteurii* (Whiffin et al., 2007; Harkes et al., 2010), can effectively promote crystallization of CPC after injection of an acidic reaction mixture with little precipitation into soil and rock (e.g., Fig. 4 C-b, B-d, and Fig. 5 D-c).

In the case of 1.5 M CN (Fig. 4 A-d, B-d, C-d, and D-d), the pH of the reaction mixture was below 4 even at the maximum PPR. This shows that if calcium is saturated, CPC can be precipitated in acidic conditions, under which the solubility of CPC is higher. Some peat soils, which are typically poor ground, show acidic properties due to the presence of humic acid (Reddy and DeLaune, 2008). The above results demonstrate the possibility of applying the CPC grout to such a soil. As the solubility of CPC is also higher in alkaline regions around pH 12, a high concentration of calcium can be achieved in such alkaline conditions (Takagi et al., 1998). The mechanism proposed by Kawasaki et al. (2006), of utilizing acidification by carbon dioxide from yeasts, may precipitate a large amount of CPC if an alkaline stock solution is initially used. In this case, it is necessary to study the utilization and activation of alkali-tolerant yeasts and bacteria.

The viscosity of the reaction mixture (CN and MAP) was 2.5 cps and approximately equivalent to that of chrome-lignin grout, which is a conventional grout (Karol, 2003). In contrast, the use of DAP instead of MAP in combination with CN increased the viscosity up to ~500 cps. This result suggests that CPC reaction mixture containing CN has suitable injectability and the potential to control the

permeability through the cracks and voids in the ground. The viscosities of the reaction mixtures of CA with MAP and of CA with DAP were similar (~100 cps). Considering that their viscosities correspond to the viscosity of a high concentration of silicate, the MAP:CA and DAP:CA solutions might show effective penetrability for soil types ranging from medium sand to fine gravel, as suggested by Karol (2003).

4.2 Compressive strength imparted by CPC

The most suitable combination of AP and calcium stock solution concentrations for improving the strength of the UCS test piece was a DAP:CA ratio of 1.5 M:0.75 M (Fig. 7 F), for which the UCS reached a maximum of 63.5 kPa. In addition, a clear peak around 1.6% was recognized in the stress (σ)-strain (ε) curve of this combination, in contrast to that of other combinations (Fig. 8). In contrast, all UCS values of the test pieces subjected to CN treatment were below 20 kPa and showed no significant trends (Fig. 7 A-C). SEM images of test pieces subjected to CA treatment showed whisker-like crystal formation among particles of Toyoura sand (Fig. 9). It has been reported that HA whiskers are formed by adding an acetic acid solution to amorphous calcium phosphate (Toyama et al., 2001). In Portland cement, the formation of ettringite, which shows whisker-like crystals, promotes solidification and increases strength (Park, 2000, Sakai et al., 2004). These results suggest that the strength of the test pieces subjected to CA treatment in this study might increase if

whisker-like HA crystals are formed within them. In addition, they show that CA would be a potent candidate calcium stock solution in applications of CPC grout. In contrast, plate-like crystals were formed in test pieces treated with CN (Fig. 9). Zhang et al. (2009) reported that plate-like HA formed in cases where CN was used as the calcium stock solution. There are a few CPCs, e.g., octacalcium phosphate (Wang et al., 2004) and DCP (dicalcium phosphate) (Toyama et al., 2001), whose precipitation leads to plate-like crystals. Non-HA CPC ultimately changes into HA (Tung, 1998). Thus, the crystal form in test pieces treated with CN may change after a long curing period, thereby increasing their strength.

In the in vitro precipitation test, the PPR of gelated precipitation was greater than that of crystal precipitation, especially in the case of phosphate solution with a molar ratio of over 0.5 M. This result is consistent with Tung's report (1998), and indicates that a hydrated compound such as gel was formed, and that this resulted in an increase in volume. According to Tung (1988), the gel precipitation is expected to be gradually crystallized to HA. These results also suggest that an appropriate selection of the type and concentration of calcium stock solution as well as the cure time can lead to greater UCS strength. It is necessary to analyze the crystal structures and to investigate the relationship between crystal formation and the mechanical properties of the test pieces in detail, including how the physical interaction occurred (e.g., the uniting of sand particles or filling of voids among sand particles by CPC).

Whiffin et al. (2007) have reported that a precipitation of calcium carbonate of at least 60 kg/m^3 is required to achieve a measurable strength improvement in a sand test piece (porosity, 37.8%) by using biogrout. Assuming that HA (Ca:PO_4:OH molar ratio of 5:3:1) precipitates maximally in the most porous of the Toyoura sand test pieces, the theoretical value of CPC precipitation in 73.3 mL of the reaction mixture was 5.5 g in the test piece shown in Fig. 8 F (porosity, 37.7%). The details of this piece, which is cemented by a DAP:CA ratio of 1.5 M:0.75 M (Fig. 5 D-c), are as follows.

(1) 0.75 M Ca is ~2.2 g of Ca mass

(2) 0.45 M PO_4 is ~3.1 g of PO_4 mass

(3) 0.15 M OH is ~0.2 g of OH mass

The volume of the Toyoura sand test piece was 194.59 cm^3; therefore, the proportionate CPC precipitation mass for a volume of 1 m^3 is 28.3 kg. This means that the CPC grout attained a UCS of 63.5 kPa by a relatively low amount of CPC precipitation. A surplus of phosphate may exist in the pore water of the test pieces treated with CA because HA has a calcium-phosphorus molar ratio of 1.67 (Table 1). This suggests that multiple injections of calcium stock solution increase HA precipitation and induce the strengthening of test pieces, as described previously (Harkes et al., 2010).

In this study, we begin by focusing on the development of novel grout material intended for soil materials (sand, in this study) and assume that the phosphate solution and calcium solution are mixed

just before injection or that they are mixed in the ground after being sequentially injected. The procedure for mixing them might be formulated based on the viscosity of the reaction mixture, the PPR of CPC precipitation, and the precipitation status over time for a particular combination of stock solutions. It is also necessary to conduct a detailed evaluation of the relationship between the UCS and the rate of stiffening because temporal variation in the UCS over the long term may prove to be one of the most important parameters in determining the applicability of CPC.

4.3 Application of knowledge in and collaboration with medical and dental science

The feasibility of improving the compressive strength was examined by forming CPC with only solutions that can be conveniently handled during practical application. Chow (1991) reported that the utilization of CPC seed crystal caused the strengthening of HA in CPC solution. In particular, they pointed out that utilization of a powder mixture of tetracalcium phosphate and DCP led to a stronger HA with the greatest purity. Their pastes also possessed the properties of self-setting and biocompatibility (Chow, 1991).

Research on CPC paste has established that a maximum compressive strength of 56 MPa can be obtained with a mixture of DCP and α-TCP pastes and a seed crystal of calcium carbonate; this is substantially greater than the compressive strength of 35 MPa obtained without the seed (Fernandez et al., 1998). This observation shows that the presence of the calcium carbonate seed crystal can

supplement the effect of strength reinforcement, as is the case for the CPC grout studied here. Co-existing ions (e.g., magnesium ions) with in situ pore water change the form of the CPC crystal (Cheng and Pritzker, 1983), and the compressive strength of HA is increased by the co-existence of bone marrow cells and CPC (Vuola et al., 1998). These observations suggest that the effective utilization of ionic and/or organic materials can be an important method for strength reinforcement in the geotechnical field.

Nowadays, clinical breakthroughs are made daily in the medical and dental sciences; these include, among others, the enhancement of the injectable (Bohner and Baroud, 2005; Habib et al., 2008), biocompatibility, and self-setting properties of CPC paste by organic matter (Maruyama and Ito, 1996) as well as the development of novel apatite blocks (Tas, 2008). The injectability of CPC grout is also one of the most important factors in its application to natural soils and rocks with minute cracks. The medical and dental sciences have accrued an extensive amount of fundamental knowledge regarding CPC.

5. Conclusion

This study examined the feasibility of a new rock grout material comprised of CPC. A candidate cement that increased the compressive strength of the sand test piece with time was found by evaluating the effect of pH, the type of phosphate and calcium stock solutions, and the component

ratios of the phosphate stock solution on the PPR of CPC. Although only chemical reactions for CPC precipitation were examined, the results of this study showed that CPCs have sufficient potential for use as:

(1) chemical grouts because of their self-setting property and

(2) biogrouts because of their crystal structure and pH dependence of precipitation.

Changes in the concentration of the reaction mixture were not reflected simplistically in the strength of the sand test pieces. In the future, additional tests aimed at determining the strength imparted by CPC are needed to better understand the underlying mechanical processes and facilitate practical application. The relationship between the strength and the various CPC precipitation parameters (concentration and pH of reaction mixture, cure time, and so on) should be examined in further detail, as continued research is needed to identify the process or processes that link crystal precipitation to the increase in strength. Furthermore, shearing and permeability tests using pieces cemented by CPC should be conducted in addition to the compression strength test to evaluate the applicability of CPCs for purposes such as permeability control and reinforcement of ground soil and rock.

6. Acknowledgement

We are grateful to Shimeno Aoi of Hokkaido University for taking the SEM images of CPC.

References

Bohner, M., Baroud, G., 2005. Injectability of calcium phosphate pastes. Biomaterials 26, 1553–1563.

Bohner, M., Doebelin, N., Baroud, G., 2006. Theoretical and experimental approach to test the cohesion of calcium phosphate pastes. Eur. Cells Mater. 12, 26–35.

Cheng P.-T., Pritzker, K.P.H., 1983. Solution Ca/P ratio affects calcium phosphate crystal phases. Calcif. Tissue Int. 35, 596–601.

Chow, L.C., 1991. Development of self-setting calcium phosphate cements. The Centennial Memorial Issue of Ceram. Soc. Japan 99, 954–964.

De Muynck, W., De Belie, N., Verstraete, W., 2010. Microbial carbonate precipitation in construction materials: A review. Ecol. Eng. 36, 118–136.

DeJong J.T., Mortensen, B.M., Martinez, B.C., Nelson, D.C., 2010. Bio-mediated soil improvement. Ecol. Eng. 36, 197–210.

Dorozhkin, S.V., Epple, M., 2002. Biological and medical significance of calcium phosphates. Angew. Chem. Int. Ed. 41, 3130–3146.

Fernández, E., Gil, F.J., Best, S.M., Ginebra, M.P., Driessens, F.C.M., Planell, J.A., 1998. Improvement of the mechanical properties of new calcium phosphate bone cements in the $CaHPO_4$-α-$Ca_2(PO_4)_2$ system: Compressive strength and microstructural development. J. Biomed.

Mater. Res. 41, 560–567.

Ginebra, M.P., Fernández, E., De Maeyer, E.A.P., Verbeeck, R.M.H., Boltong, M.G., Ginebra, J., Driessens, F.C.M., Planell, J.A., 1997. Setting reaction and hardening of an apatitic calcium phosphate cement. J. Dent. Res.76, 905–912.

Ginebra, M.P., Traykova, T., Planell, J.A., 2006. Calcium phosphate cements as bone drug delivery systems: A review. J. Control. Release 113, 102–110.

Habib, M., Baroud, G., Gitzhofer, F., Bohner, M., 2008. Mechanisms underlying the limited injectability of hydraulic calcium phosphate paste. Acta Biomater. 4, 1465–1471.

Harkes, M.P., van Paassen, L.A., Booster, J.L., Whiffin, V.S., van Loosdrecht, M.C.M., 2010. Fixation and distribution of bacterial activity in sand to induce carbonate precipitation for ground reinforcement. Ecol. Eng. 36, 112–117.

Kagakubinran (Ed.) Chemical Society of Japan (Table of Chemical and Physical data), 4th Edition, Maruzen, Tokyo, 1993 (in Japanese).

Karol, R.H., 2003. Chemical grouting and soil stabilization, 3rd Ed., CRC Press, Boca Raton, FL.

Kawasaki, S., Murao, A., Hiroyoshi, N., Tsunekawa, M., Kaneko, K., 2006. Fundamental study on novel grout cementing due to microbial metabolism. J. Japan Soc. Eng. Geol. 47, 2–12 (in Japanese, with English abstract).

Kawasaki, S., Ogata, S., Hiroyoshi, N., Tsunekawa, M., Kaneko, K., Terashima, R., 2010. Effect of

temperature on precipitation of calcium carbonate using soil microorganisms. J. Japan Soc. Eng. Geol. 51, 10–18 (in Japanese, with English abstract).

Mann, S., 1988. Molecular recognition in biomineralization. Nature 332, 119–124.

Mann, S., 1993. Molecular tectonics in biomineralization and biomimetic materials chemistry. Nature 365, 499–505.

Martin R.I., Brown, P.W., 1995. Mechanical properties of hydroxyapatite formed at physiological temperature. J. Mater. Sci.: Mater. Med. 6, 138–143.

Maruyama, M., Ito, M., 1996. *In vitro* properties of a chitosan-bonded self-hardening paste with hydroxyapatite granules. J. Biomed. Mater. Res. 32, 527–532.

Park, C.-K., 2000. Hydration and solidification of hazardous wastes containing heavy metals using modified cementitious materials. Cement. Concr. Res. 30, 429–435.

Reddy, K.R., DeLaune, R.D., 2008. Biogeochemistry of wetlands: science and applications. CRC Press, Boca Raton, FL.

Sakai, E., Nikaido, Y., Itoh, T., Daimon, M., 2004. Ettringite formation and microstructure of rapid hardening cement. Cement. Concr. Res. 34, 1669–1673.

Takagi, S., Chow, L.C., Ishikawa, K., 1998. Formation of hydroxyapatite in new calcium phosphate cements. Biomaterials 19, 1593–1599.

Tas A.C., 2008. Preparation of porous apatite granules from calcium phosphate cement. J. Mater.

Sci.: Mater. Med. 19, 2231–2239.

Terajima, R., Shimada, S., Oyama, T., Kawasaki, S., 2009. Fundamental study of siliceous biogrout for eco-friendly soil improvement. J. Geotech. Geoenv. Eng. JSCE 65, 120–130 (in Japanese, with English abstract).

The Merck Index, 2001. Merck & Co., Inc, NJ.

Toyama, T., Ohshima, A, Yasue, T., 2001. Hydrothermal synthesis of hydroxyapatite whisker from amorphous calcium phosphate and effect of carboxylic acid. J. Ceram. Soc. Japan 109, 232–237 (in Japanese, with English abstract).

Tung, M.S., 1998. Calcium phosphates: structure, composition, solubility, and stability, in: Zahid, A. (Eds.), Calcium phosphates in biological and industrial systems. Kluwer Academic Publishers, Norwell, pp. 1–19.

van Paassen, L.A., Harkes, M.P., van Zwieten, G.A., van der Zon, W.H., van der Star, W.R.L., van Loosdrecht, M.C.M., 2009. Scale up of BioGrout: a biological ground reinforcement method. 2009. Proc. 17th Int. Conf. Soil Mech. Geotech. Eng. 2328–2333.

Vuola, J., Taurio, R., Göransson, H., Asko-sljavaara, S., 1998. Compressive strength of calcium carbonate and hydroxyapatite implants after bone-marrow-induced osteogenesis. Biomaterials 19, 223–227.

Wang, J., Layrolle, P., Stigter, M., de Groot, K., 2004. Biomimetic and electrolytic calcium

phosphate coatings on titanium allow: physicochemical characteristics and cell attachment. Biomaterial. 25, 583–592.

Whiffin, V.S., van Paassen, L.A., Harkes, M.P., 2007. Microbial carbonate precipitation as a soil improvement technique. Geomicrobiol. J. 24, 417–423.

Wilson, E.E., Yound, C.V., Holway, D.A., 2010. Predation or scavenging? Thoracic muscle pH and rates of water loss reveal cause of death in arthropods. J. Exp. Biol. 213, 2640–2646.

Zhang, H.-B., Zhou K.-C., Li, Z.-Y., Huang S.-P., 2009. Plate-like hydroxyapatite nanoparticles synthesized by the hydrothermal method. J. Phys. Chem. Solid. 70, 243–248.

Table 1

Properties of biologically relevant calcium orthophosphates (Dorozhkin and Epple, 2002).

Ca/P ratio	Compound	Abbreviation	Formula
0.5	Monocalcium phosphate monohydrate	MCPM	$Ca(H_2PO_4)_2 \cdot H_2O$
0.5	Monocalcium phosphate anhydrate	MCPA	$Ca(H_2PO_4)_2$
1.0	Dicalcium phosphate dihydrate	DCPD	$CaHPO_4 \cdot 2H_2O$
1.0	Dicalcium phosphate anhydrate	DCPA	$CaHPO_4$
1.33	Octacalcium phosphate	OCP	$Ca_8(HPO_4)_2(PO_4)_4 \cdot 5H_2O$
1.5	A-tricalcium phosphate	α-TCP	$\alpha\text{-}Ca_3(PO_4)_2$
1.5	B-tricalcium phosphate	β-TCP	$\beta\text{-}Ca_3(PO_4)_2$
1.2–2.2	Amorphous calcium phosphate	ACP	$Ca_x(PO_4)_y \cdot nH_2O$
1.5–1.67	Calcium-deficient hydroxyapatite	CDHA	$Ca_{10-x}(HPO_4)_x(PO_4)_{6-x}(OH)_{2-x}$ $(0<x<1)$
1.67	Hydroxyapatite	HA	$Ca_{10}(PO_4)_6(OH)_2$
2.0	Tetracalcium phosphate	TTCP	$Ca_4(PO_4)_2O$

Table 2

Physical characteristics of Toyoura sand.

Soil particle density, ρ_s (g/cm^3)	2.64
Minimum density, ρ_{min} (g/cm^3)	1.335±0.005
Maximum density, ρ_{max} (g/cm^3)	1.645±0.010
Maximum void ratio, e_{max}	0.973
Minimum void ratio, e_{min}	0.609
Mean grain size, D_{50} (mm)	0.17
10% diameter on grain size diagram, D_{10} (mm)	0.11
Fine fraction content, Fc (%)	0

Figure 1

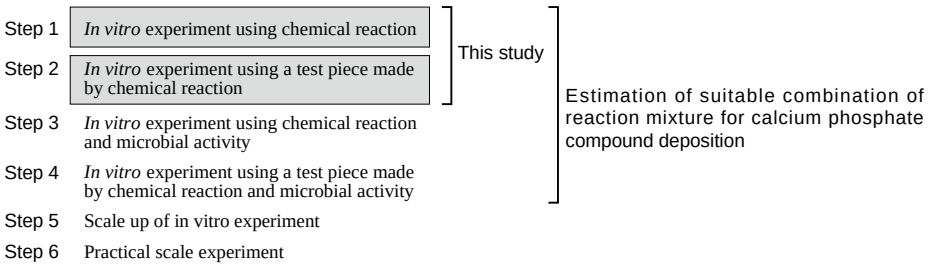
Step 1
In vitro experiment using chemical reaction
Step 2
In vitro experiment using a test piece made by chemical reaction
This study
Step 3
In vitro experiment using chemical reaction and microbial activity
Step 4
In vitro experiment using a test piece made by chemical reaction and microbial activity
Step 5
Scale up of in vitro experiment
Step 6
Practical scale experiment
Estimation of suitable combination of reaction mixture for calcium phosphate compound deposition

Figure 2

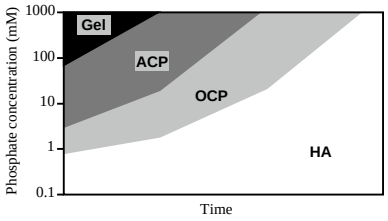
Phosphate concentration (mM)
1000
100
10
1
0.1
Gel
ACP
OCP
HA
Time

Figure 3

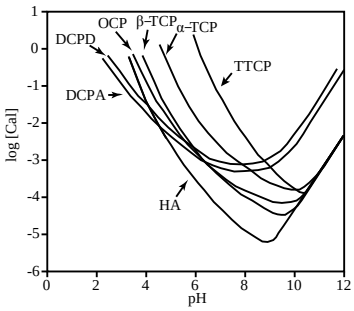
DCPD
OCP
β–TCP
α–TCP
TTCP
DCPA
HA
log [Cal]
pH
1
0
-1
-2
-3
-4
-5
-6
0
2
4
6
8
10
12

Figure 4

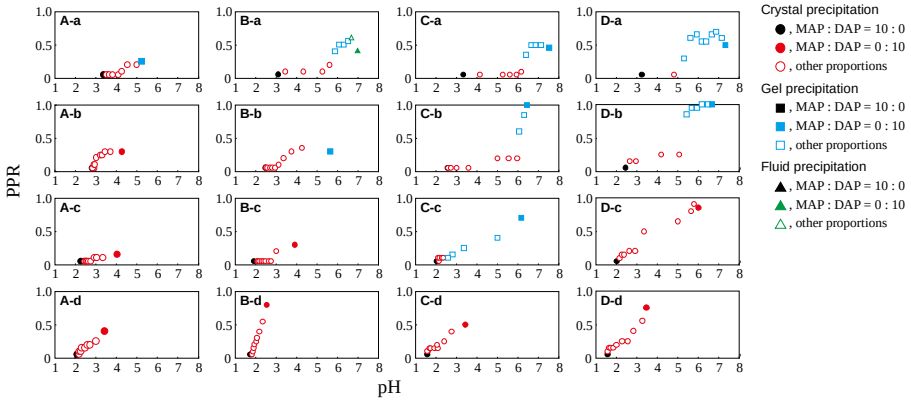
A-a
B-a
C-a
D-a
A-b
B-b
C-b
D-b
A-c
B-c
C-c
D-c
A-d
B-d
C-d
D-d
PPR
pH
Crystal precipitation
, MAP : DAP = 10 : 0
, MAP : DAP = 0 : 10
, other proportions
Gel precipitation
, MAP : DAP = 10 : 0
, MAP : DAP = 0 : 10
, other proportions
Fluid precipitation
, MAP : DAP = 10 : 0
, MAP : DAP = 0 : 10
, other proportions

Figure 5

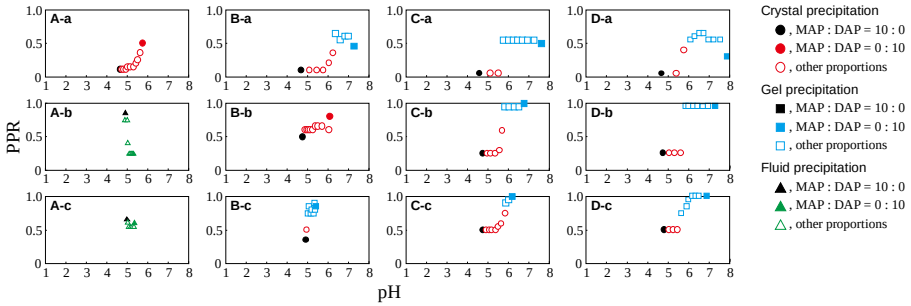
A-a
B-a
C-a
D-a
A-b
B-b
C-b
D-b
A-c
B-c
C-c
D-c
PPR
pH
Crystal precipitation
, MAP : DAP = 10 : 0
, MAP : DAP = 0 : 10
, other proportions
Gel precipitation
, MAP : DAP = 10 : 0
, MAP : DAP = 0 : 10
, other proportions
Fluid precipitation
, MAP : DAP = 10 : 0
, MAP : DAP = 0 : 10
, other proportions

Figure 6

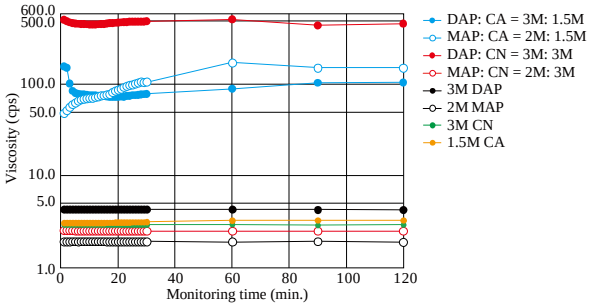
600.0
500.0
100.0
50.0
10.0
5.0
1.0
Viscosity (cps)
0
20
40
60
80
100
120
Monitoring time (min.)
DAP: CA = 3M: 1.5M
MAP: CA = 2M: 1.5M
DAP: CN = 3M: 3M
MAP: CN = 2M: 3M
3M DAP
2M MAP
3M CN
1.5M CA

Figure 7

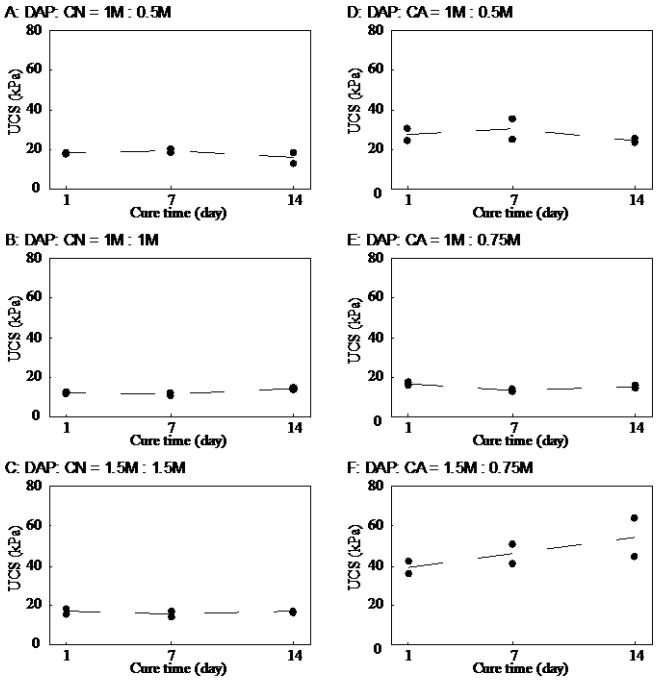
A: DAP: CN = 1M : 0.5M
D: DAP: CA = 1M : 0.5M
B: DAP: CN = 1M : 1M
E: DAP: CA = 1M : 0.75M
C: DAP: CN = 1.5M : 1.5M
F: DAP: CA = 1.5M : 0.75M
UCS (kPa)
0
20
40
60
80
1
7
14
Cure time (day)

Figure 8

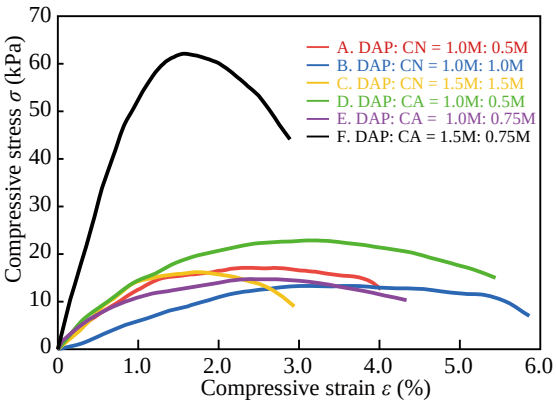
Compressive stress σ (kPa)
70
60
50
40
30
20
10
0
0
1.0
2.0
3.0
4.0
5.0
6.0
Compressive strain ε (%)
A. DAP: CN = 1.0M: 0.5M
B. DAP: CN = 1.0M: 1.0M
C. DAP: CN = 1.5M: 1.5M
D. DAP: CA = 1.0M: 0.5M
E. DAP: CA = 1.0M: 0.75M
F. DAP: CA = 1.5M: 0.75M

Figure 9

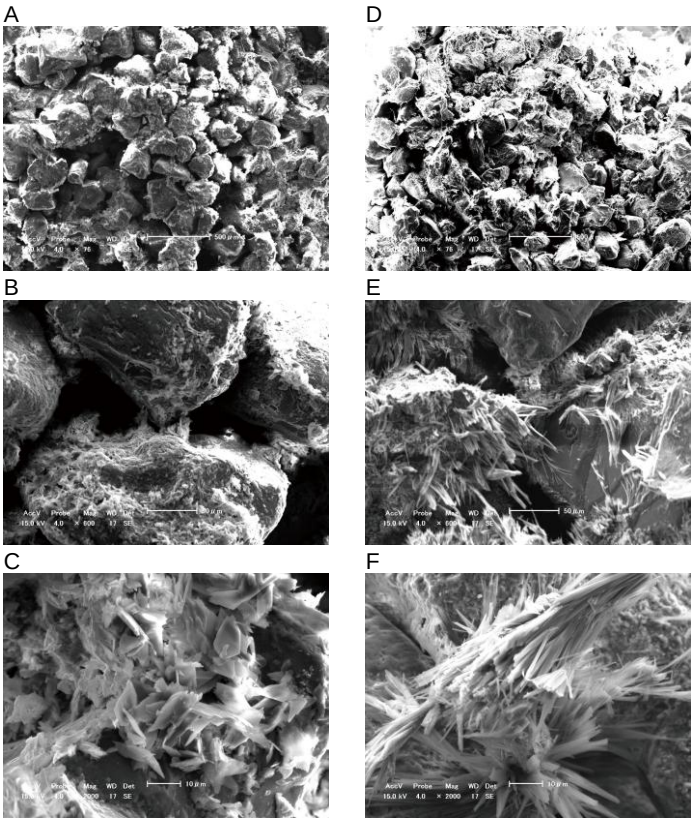

Figure 10

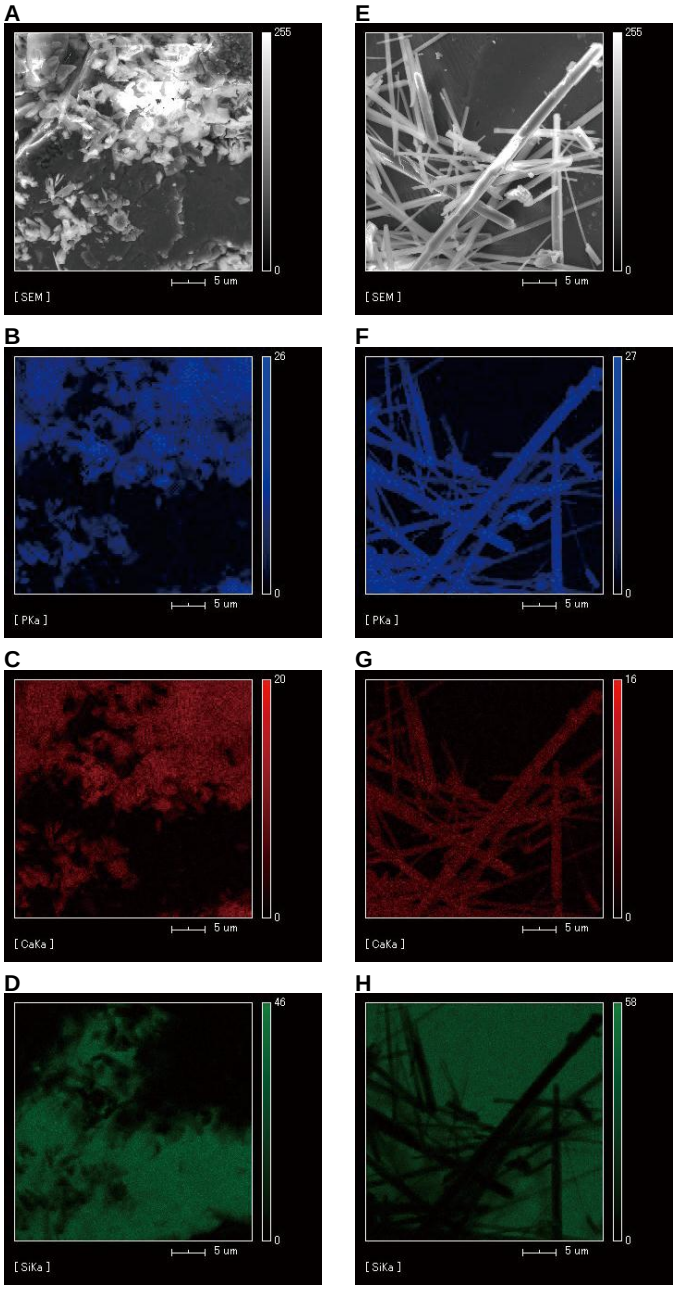
A
255
0
5 um
[SEM]
E
255
0
5 um
[SEM]
B
26
0
5 um
[PKa]
F
27
0
5 um
[PKa]
C
20
0
5 um
[CaKa]
G
16
0
5 um
[CaKa]
D
46
0
5 um
[SiKa]
H
58
0
5 um
[SiKa]

Figure Captions

Fig. 1. Flowchart of the study. The steps carried out in this study are highlighted in gray.

Fig. 2. Formation, stability, and hydrolysis of calcium phosphates as a function of phosphate concentration (log(P)) in solutions of amorphous phosphate (ACP) at neutral pH. OCP, octacalcium phosphate; HA, hydroxyapatite. The figure is adapted from Tung (1998).

Fig. 3. Solubility phase diagrams for the ternary system, $Ca(OH)_2$-H_3PO_4-H_2O, at 25 °C, showing the solubility isotherms of $CaHPO_4$ (DCPA), $CaHPO_4 \cdot 2H_2O$ (DCPD), $Ca_8H_2(PO_4)_6 \cdot 5H_2O$ (OCP), α-$Ca_3(PO4)_2$ (α-TCP), β-$Ca_3(PO_4)_2$ (β-TCP), $Ca_4(PO_4)_2O$ (TTCP), and $Ca_{10}(PO_4)_6 \cdot (OH)_2$, (HA). The figure is adapted from Tung (1998).

Fig. 4. Relationship between the proportion of CPC precipitation volume of reaction mixture (PPR) and pH for calcium nitrate. The value is represented as the proportion of the precipitation volume to the entire volume of the reaction mixture (4 mL). Ammonium phosphate solution was used as an initial pH regulator by mixing monoammonium phosphate (MAP) solution and diammonium phosphate (DAP) solution in 11 mixing proportions (10:0 to 0:10). Capital (ammonium phosphate) and lowercase letters (calcium nitrate) in each figure represent the final concentrations (0.1 M (A, a),

0.5 M (B, b), 1.0 M (C, c), and 1.5 M (D, d)) of each solution in the mixture. In vitro precipitation was carried out by mixing equal volumes of ammonium phosphate and calcium nitrate solutions. CPC precipitation was classified into three states based on visual observation.

Fig. 5. Relationship between the proportion of CPC precipitation volume of reaction mixture (PPR) and pH using calcium acetate. The value is represented as the proportion of CPC precipitation volume to the entire volume of the reaction mixture (4 mL). Ammonium phosphate solution was used as an initial pH regulator by mixing monoammonium phosphate (MAP) and diammonium phosphate (DAP) solutions in 11 mixing proportions (10:0 to 0:10). Capital (ammonium phosphate) and lowercase letters (calcium acetate) in each figure represent the final concentrations (0.1 M (A, a), 0.5 M (B, b), 0.75 M (c), 1.0 M (C) and 1.5 M (D)) of each solution in the mixture. In vitro precipitation was carried out by mixing equal volumes of ammonium phosphate and calcium acetate solutions. Precipitation of CPC was classified into three states based on visual observation.

Fig. 6. Viscosities of single stock solutions and reaction mixtures of phosphate and/or calcium.

Fig. 7. Temporal variations in unconfined compressive strength (UCS) of Toyoura sand test pieces cemented by CPCs. Mixing concentrations of diammonium phosphate and calcium solutions

(calcium nitrate (A, B, C) and calcium acetate (D, E, F)) for mixture of each grout: A, 1 M:0.5 M; B, 1 M:1 M; C, 1.5 M:1.5 M; D, 1 M:0.5 M; E, 1 M:0.75 M; F, 1.5 M:0.75M. The dashed line represents the change in the average of two measurements.

Fig. 8. Compressive stress (σ)-compressive strain (ε) curves of test pieces cemented by CPC.

Fig. 9. Scanning electron microscope (SEM) images of Toyoura sand test piece cemented by diammonium phosphate and calcium nitrate (A, B, and C) or calcium acetate (D, E, and F). A and D, ×76; B and D, ×600; and C and F, ×2000. An accelerating voltage of 15 kV was used for the observations. Bars represent 500, 50, and 10 mm in A and D, B and E, and C and F, respectively.

Fig. 10. Energy dispersive X-ray (EDX) fluorescence spectrometer images of Toyoura sand test piece cemented by diammonium phosphate and calcium nitrate (A, B, C, and D) or calcium acetate (E, F, G, and H). A and E, SEM images; B and F, distribution of phosphorous; C and G, distribution of calcium; and D and H, distribution of silicon. Intensity of colors shows the relative amount of atoms in each image. Bars represent 5 μm.